Effects of Substitution on the Singlet−Triplet Energy Splittings and Ground-State Multiplicities of *m*-Phenylene-Based Diradicals: A Density Functional Theory Study

Ganbing Zhang, Shuhua Li,* and Yuansheng Jiang

Department of Chemistry, Institute of Theoretical and Computational Chemistry, Lab of Mesoscopic Materials Science, Nanjing University, Nanjing 210093, People's Republic of China

Received: December 13, 2002

Unrestricted density functional calculations with spin-projection procedures have been performed for a series of *m*-phenylene-bridged diradicals to investigate the effects of substitution on the singlet−triplet (S−T) energy gaps and the ground-state multiplicities. Our calculations show that the introduction of electron-donating (or electron-withdrawing) substituents on 4,6-positions of the *m*-phenylene moiety or on the radical centers, or on both positions, generally leads to a triplet ground state, although the S−T energy gaps are smaller than that of the parent *m*-xylylene diradical to some extent. However, the simultaneous substitution of electron-donating and electron-withdrawing groups at *m*-phenylene and radical centers, and *vice versa*, will result in a singlet ground state or a very small positive S−T gap. A perturbative analysis based on the SOMO−SOMO energy splittings, the spatial distributions of SOMOs, and the population of the spin densities calculated for the triplet state has been presented to elucidate factors determining the S−T gap and ground-state multiplicity in studied diradicals.

1. Introduction

Design and synthesis of molecule-based organic ferromagnetic materials have attracted great attention both experimentally and theoretically in recent years.[1−6] Along Dougherty's scheme,[1,7]

Dougherty's scheme of magnetic interaction

magnetic molecules can be divided into two kinds of building blocks, spin-containing units (SCU), such as organic radicals or transition metals, and coupling units (CU) that connect spin sources. Ferro(antiferro)magnetic coupling units (F(A)CU) stabilize the parallel (antiparallel) configurations of spins between radical sites, leading to the high (low)-spin ground states of molecules.

Up to now, the best studied FCU is *m*-phenylene.[8−36] A large number of works for preparing high-spin organic radicals through an *m*-phenylene coupling unit have been carried out.[9−22] Many experimental and theoretical investigations on the structures of spin blocks linked by *m*-phenylene have shown that the *m*-phenylene coupler is generally effective for the realization of high-spin ground states in organic molecules,[9−36] not only for diradical molecules[10−12,13a,18a,b,20] but also for polyradicals,[13b,14−17,19a] polyionic radicals,[21] and polymer or dendrimers.[19b,26−29] As an example, *m*-xylylene has attracted much attention because it is the simplest diradical through *m*-phenylene having the triplet ground state.[30−36] The origin of its triplet ground state has been well interpreted in terms of several different models, such as the first Hund rule, the Longuet-Higgins rule,[37] the Borden−Davidson scheme,[38] and the starred/unstarred topological rule.[39] In general, *m*-phenylene connects spin carriers ferromagnetically, not only on a pair of carbon-centered radicals[10,30,31] or carbenes[11] but also on two nitrogen-centered radicals,[11b] on two nitrenes,[12] and on two nitroxyl groups,[13] even on two polarons,[21c] etc.

However, some experimental and theoretical studies indicated that *m*-phenylene does not always serve as a ferromagnetic coupling unit. Conformations of the spin sources or spin delocalization into substituents could impact the effectiveness of *m*-phenylene as a FC or even lead to the loss of ferromagnetic coupling.[24a,40] For example, several *m*-phenylene-bridged diradicals with heteroatom-based spin carriers such as dinitroxides,[41] bisphenothiazine dications,[42a] and dithioxanthyl dications,[42b] have recently been prepared and reported to prefer a singlet ground state.[41,42] These diradicals have been characterized as having the radical centers significantly twisting out of, even close to perpendicular to, the phenylene unit due to high steric hindrance.[41−42] Semiempirical UHF-AM1[42] and ab initio calculations[43] indicated that the singlet ground state is attributable to the orbital interaction between the singly occupied molecular orbitals (SOMOs) at the two radical centers and the σ and σ^* orbitals of the *m*-phenylene moiety, which results in the lifting of the degeneracy of two SOMOs. Rajca et al. have synthesized a series of alkyl-substituted Schlenk hydrocarbons and found that most of them have robust triplet ground states.[18a,b] But one of them, the 2,4,6-trimethyl-1,3-phenylene-based diradical, was shown experimentally to have a singlet ground state with a small S−T energy gap.[44] It was believed that spin density in this diradical may delocalize more readily into the aryl substituents than the relatively hindered *m*-phenylene bridge, leading to a relatively smaller spin density in the spin coupling unit.

In general, radicals such as *m*-xylylene are very unstable with respect to dimerization or reaction with oxygen, so introduction of substituents at *m*-phenylene or at radical centers to increase the kinetic/thermodynamic stability by increasing the steric hindrance is a common strategy utilized to synthesize stable high-spin organic radicals by experimental chemists.[18−20,22,44] However, the introduction of substituents may diminish the S−T

* To whom correspondence should be addressed. E-mail: shuhua@netra.nju.edu.cn.

10.1021/jp022596d CCC: $25.00
Published on Web 06/26/2003

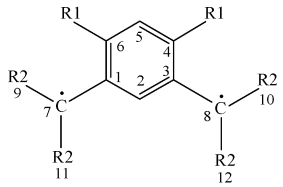

molecules	R1	R2	molecules	R1	R2	molecules	R1	R2
1	H	H	**10**	H	CHO	**19**	CN	CN
2	H	NMe_2	**11**	H	CN	**20**	NH_2	NO_2
3	H	NH_2	**12**	H	NO_2	**21**	OMe	NO_2
4	H	CH_3	**13**	NH_2	H	**22**	NO_2	NO_2
5	H	OMe	**14**	OMe	H	**23**	NO_2	NH_2
6	H	OH	**15**	CN	H	**24**	CN	NH_2
7	H	F	**16**	NO_2	H	**25**	OMe	NH_2
8	H	Cl	**17**	NH_2	CN	**26**	NH_2	NH_2
9	H	COOH	**18**	OMe	CN			

Figure 1. Selected molecules (hydrogen atoms are omitted for clarity).

energy difference or even lead to the low-spin ground state. For example, trimethylenemethane (TMM) is well-known to have a triplet ground state;[45] its derivative with the substitution of oxygen for one methylene of TMM, oxyallyl (OXA), was found to have nearly degenerate singlet and triplet states,[46] but the alkyl derivatives of OXA were shown to have unequivocal singlet ground states.[47a] The alkyl or heteroatom substitutions in TMM have been thoroughly investigated theoretically.[47b−d] It was found that one of the two SOMOs in the parent diradical is selectively stabilized by the $\sigma-\pi$ interaction; thus the singlet state is more stabilized than the triplet state, and even becomes the ground state.[35,48]

To our knowledge, for the *m*-phenylene-bridged diradical systems with carbon spin carriers, the effects of introducing electronic donor or acceptor substituents at *m*-phenylene moiety or the radical centers on their magnetic behaviors are still less studied.[18−19,22] Thus, theoretical investigations on substitution effects on the S−T gaps of *m*-phenylene-bridged diradicals will provide very useful references for experimental chemists. In this paper we undertake a systematic theoretical study on the effects of various substituents on the magnetic properties of *m*-phenylene-bridged diradicals. On the basis of the parent diradical **1**, we have introduced different donor and acceptor substituents at 4,6-positions of *m*-phenylene or at the radical centers (Figure 1). As given in Figure 1, each studied diradical can be denoted as R1−B−R2, in which R1 and R2 can be a hydrogen (H), an electron donor (D), and an electron acceptor (A). For example, diradicals **2**−**12** are described by H−B−D or H−B−A, and molecules **17**, **18** and **20**, **21** belong to the D−B−A type.

The theoretical method we used in this work is density functional theory (DFT), which has become the powerful tool for calculating the electronic structures of radical systems[26−29] in recent years. Specifically, the hybrid DFT method, B3LYP,[49] is employed. For diradicals in the triplet state, unrestricted B3LYP (UB3LYP) calculations are performed, and for singlet diradicals, broken symmetry (BS)[50−53] UB3LYP calculations are carried out, followed by approximate spin projections.[52−55] DFT calculations with this approach have been shown to give the S−T gap values comparable to the results of more elaborate ab initio MO methods and experimental results for many systems.[53b,c,56−60]

2. Method of Calculation

For diradicals, its lowest singlet and triplet states are often fit to energy levels predicted by a Heisenberg model Hamiltonian $H = -2JS_a \cdot S_b$. Thus the spin-coupling constant J for diradicals is related to the singlet−triplet (S−T) energy gap, ΔE_{ST}, by $\Delta E_{ST} = 2J$, where $\Delta E_{ST} = E_S - E_T$, E_S and E_T are the total energies of the pure singlet and triplet states, respectively. The sign and magnitude of J determine the nature and the strength of magnetic interaction. A positive value of J means a triplet ground state, and thus a ferromagnetic coupling between two spins. Otherwise, a negative J indicates a singlet ground state, an antiferromagnetic behavior.

As is well-known, for lowest singlet states of diradicals, the broken symmetry solutions often have lower energies than the corresponding symmetrical solutions.[26−29,57,61] Thus the BS approach is employed. However, because the BS wave functions are often spin contaminated by higher multiplicity states, their energies should be corrected by eliminating unwanted spin states. There are several schemes for eliminating the spin contaminations in unrestricted DFT (UDFT) BS solutions, each of which leads to a procedure for computing spin-coupling constant J. Two widely used schemes were proposed by Noodleman[51a] and Davidson[51b] (ND), and Yamaguchi (Y) et al.,[52,53] which are respectively given below (we rewrite the formulas in our notation):

$$J_{ND} = \frac{E_{BS} - E_T}{S_{max}^2} \tag{1}$$

$$J_Y = \frac{E_{BS} - E_T}{\langle \hat{S}^2 \rangle_T - \langle \hat{S}^2 \rangle_{BS}} \tag{2}$$

where E_X and $\langle \hat{S}^2 \rangle_X$ (X = BS, T) denote, respectively, the total energy and the expectation value of the square of the total spin angular momentum for the broken-symmetry singlet states and triplet states by UDFT methods, and S_{max} is from $\langle \hat{S}^2 \rangle_T = S_{max}(S_{max} + 1)$, the spin size of the UDFT triplet state. In general, the UDFT triplets are slightly spin-contaminated, whereas the BS singlet states suffer from larger spin contaminations. However, the energy gap between the pure singlet state and the UDFT triplets can be estimated as $\Delta E_{ST} = \langle \hat{S}^2 \rangle_T J$ given by Ginsberg.[62] If substituting J_Y into this equation, we obtain the formula independently proposed by Yamaguchi and Houk et al.[54,55] by eliminating spin contamination of the BS singlet with the approximate spin-projection procedure.

Full geometrical optimizations and unrestricted B3LYP (UB3LYP) calculations have been performed using the GAUS-

TABLE 1: Energies (au) of the Triplet States, the Broken Symmetry Singlet States Spin-Coupling Constant *J* (kcal/mol), and the Singlet−Triplet Gaps ΔE_{ST} (kcal/mol) (after Spin Projection) at the UB3LYP/6-31G(d) Level for Selected Molecules

molecules	E_T ($\langle S^2 \rangle$)	E_{BS} ($\langle S^2 \rangle$)	J_{ND}	J_Y	ΔE_{ST}
1	−309.585129 (2.0709)	−309.574418 (1.0123)	6.42	6.35	13.15
1[a]	−308.577985 (2.6425)	−308.565070 (1.0465)	5.62	5.08	13.42
2	−845.452351 (2.0432)	−845.446104 (0.9945)	3.81	3.74	7.64
3	−531.001964 (2.0445)	−530.994251 (0.9951)	4.70	4.61	9.43
4	−466.852243 (2.0592)	−466.844632 (1.0114)	4.59	4.56	9.39
5	−767.680388 (2.0590)	−767.670686 (1.0080)	5.86	5.79	11.93
6	−610.454070 (2.0596)	−610.443902 (1.0067)	6.14	6.06	12.48
7	−706.518686 (2.0646)	−706.509183 (1.0101)	5.72	5.66	11.68
8	−2147.961491 (2.0604)	−2147.953511 (1.0111)	4.81	4.77	9.83
9	−1063.855087 (2.0533)	−1063.848278 (0.9949)	4.13	4.04	8.29
10	−762.856995 (2.0635)	−762.853092 (1.0275)	2.35	2.36	4.88
11	−678.559362 (2.0671)	−678.554576 (1.0143)	2.87	2.85	5.90
12	−1127.532116 (2.0590)	−1127.525796 (0.9942)	3.82	3.73	7.67
13	−420.292151 (2.0586)	−420.286635 (0.8834)	3.33	2.95	6.06
14	−538.630476 (2.0614)	−538.621940 (0.9714)	5.15	4.91	10.13
15	−494.072704 (2.0757)	−494.063197 (0.9809)	5.68	5.45	11.31
16	−718.573627 (2.0650)	−718.570343 (0.8482)	1.98	1.69	3.50
17	−789.276183 (2.0367)	−789.287311 (0.3508)	−6.82	−4.14	−8.44
18	−907.605205 (2.0507)	−907.605732 (0.8443)	−0.32	−0.27	−0.56
19	−863.011542 (2.0775)	−863.006062 (1.0344)	3.27	3.30	6.85
20	−1238.255780 (2.0230)	−1238.268236 (0.0650)	−7.70	−3.99	−8.08
21	−1356.581832 (2.0336)	−1356.581362 (0.8665)	0.29	0.25	0.51
22	−1536.483787 (2.0598)	−1536.481233 (0.9955)	1.54	1.51	3.10
23	−940.007011 (2.0208)	−940.037964 (0.0000)	−19.16	−9.61	−19.42
24	−715.505577 (2.0301)	−715.511004 (0.3468)	−3.34	−2.02	−4.11
25	−760.042299 (2.0446)	−760.033248 (1.0089)	5.52	5.48	11.21
26	−641.702048 (2.0451)	−641.696691 (0.8718)	3.26	2.87	5.86

[a] UCCSD/6-31G(d)//UB3LYP/6-31G(d) for **1**.

SIAN-98 program[63] for triplet and BS singlet states of all studied molecules. For some molecules with several minimum structures, we have tried efforts to locate the global minimum structure for each species. For each structure a frequency calculation is done to verify whether it is a minimum or a saddle point. Single-point ROB3LYP calculations at UB3LYP-optimized geometries for triplets of all selected molecules are also carried out for analyzing the singly occupied molecular orbitals. For all atoms in studied molecules, the standard 6-31G-(d) basis set has been used.

3. Results and Discussion

First, for verifying the reliability of the selected computational method, we carry out UB3LYP calculations for *m*-xylylene (**1**), which has been extensively studied experimentally and theoretically.[28−36] Single-point energy calculations at the UB3LYP-optimized geometries for **1** are also undertaken by using sophisticated UCCSD method for the purpose of comparison. As shown in Table 1, the UB3LYP calculations give $\Delta E_{BS-T} = 6.72$ kcal/mol for **1**; after approximate spin projection we obtain $\Delta E_{ST} = 13.15$ kcal/mol, being very close to our computed value of 13.42 kcal/mol at the UCCSD/6-31G(d) level. Previous research[64] indicated that the spin-projection procedure overcorrects the singlet energies of diradical species to some extent, and the true singlet energy lies between the spin-contaminated and spin-projected singlet energies. So our calculated values are reasonably comparable to the experimental value 9.6 ± 0.2 kcal/mol measured by Wenthold et al.[31] Thus, the combination of the BS UB3LYP approach and approximate spin-projection procedure is a practical and reliable theoretical tool for describing the lowest singlet and triplet states of the selected diradicals.

Figure 2 shows the optimized geometries for the triplet states of all the molecules. The geometries of the BS singlet states are very similar to those of the corresponding triplet states, and thus are not shown for simplicity. As shown in Figure 2, the parent diradical **1** has a planar geometry, and so do the molecules **7**, **8**, **11**, **15**, **17**, and **19**. For all other molecules, the aromatic ring and the two radical centers are almost coplanar, but in some species substituents twist out of the aromatic plane at various degrees. Obviously, for each species the optimized geometry results from the competition between π-conjugation and steric repulsion. It is well-known that π-conjugation favors a planar structure, but the steric repulsion between the *m*-phenylene coupler and the substituents, or between adjacent substituents, tends to introduce the nonplanarity for the molecule. Due to the competition between π-conjugation and steric repulsion, the species with larger substituents such as $-NO_2$ and $-NH_2$ at two radical centers usually has several minimum structures. We have performed full geometry optimizations starting with different initial structures for these species, and obtained the global minimum structure for each species, as displayed in Figure 2. Generally, for species with substituents at radical centers, the atoms of substituents bonded to the radical center are out of the aromatic plane to some extent. For example, at each radical site the nitrogen atoms of two amino groups twist out of plane by 17.3° and 10.6°, respectively, in species **3**, and similar distortions are found for its analogous species **23**−**26**. The nitrogen atoms of two nitro groups at each radical center of species **20** rotate out of plane by 30.0° and 22.9°, respectively, and similar distortions occur in compounds **21** and **22**. Especially, for species with nitro substituents at two radical centers, the torsion angle between the NO_2 plane and the aromatic plane is also an important structural parameter. The smaller the torsion angle is, the stronger the π conjugation effect between the NO_2 group and the aromatic ring is, and the stronger the steric repulsion between two NO_2 groups is. For instance, in **12** (C_2 symmetry), the torsion angle is about 41° for both nitro groups at one radical site. Thus the π delocalization effect between two NO_2 groups and the aromatic ring is significantly reduced compared to that in the hypothetical planar structure (which is actually not a minimum structure). Interestingly, the

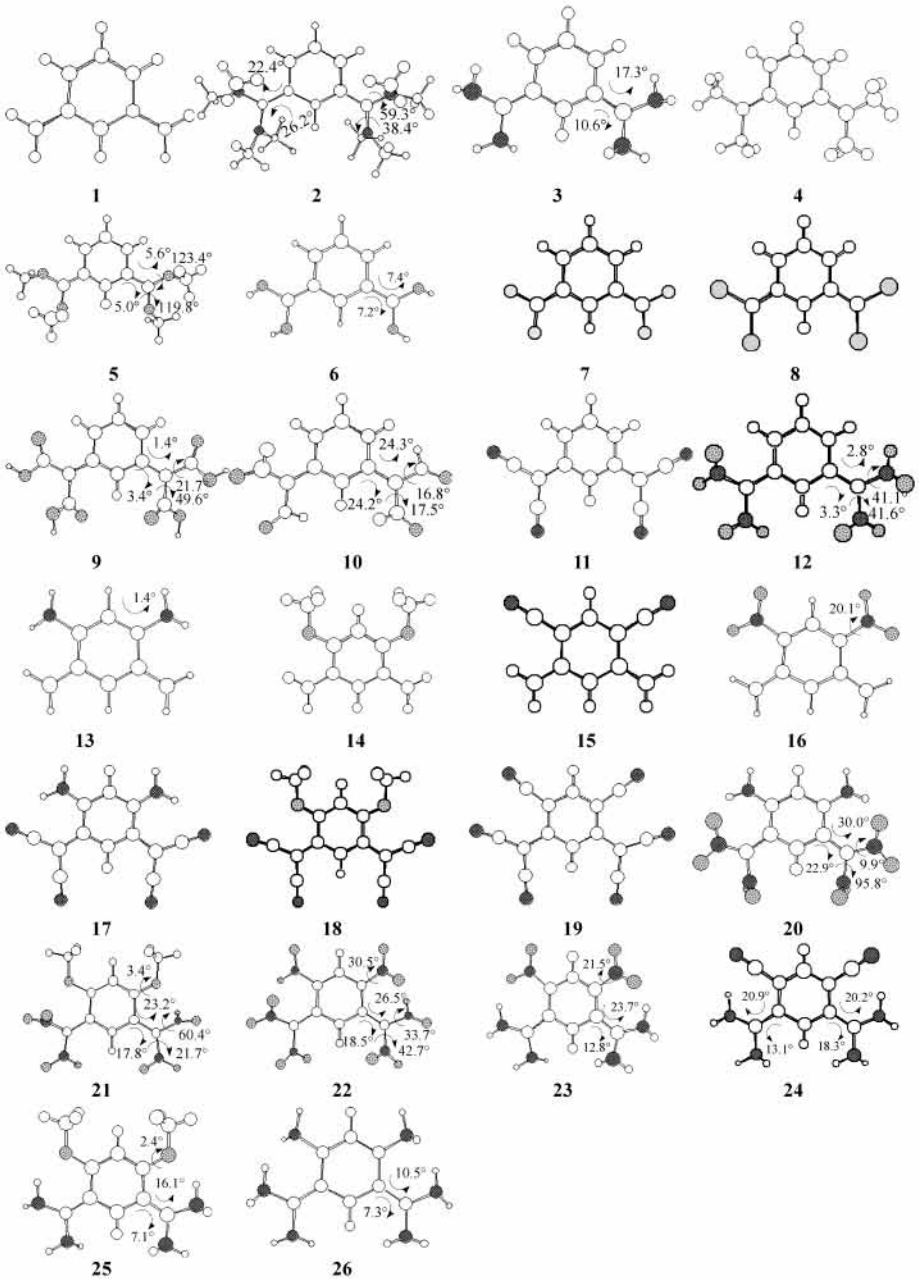

Figure 2. UB3LYP-optimized geometries for the triplet states of all selected molecules.

torsion angle between the NO_2 plane and the aromatic plane at the radical centers is found to vary significantly with changing the R1 substituents. For homologous series **20**−**22**, the torsion angle is 9.9° and 95.8° for **20** with R1 = NH_2, 60.4° and 21.7° for **21** with R1 = OMe, 33.7°, and 42.7° for **22** with R1 = NO_2. On the other hand, for species with R1 substituents being NO_2, the NO_2 plane also twists out of the aromatic plane by various degrees. For example, the NO_2 plane is out of the aromatic plane by 30.5° in **22**, and by 21.5° in **23**.

For all studied molecules, the calculated energies of triplet states and the BS singlet states, the S−T energy gaps, ΔE_{ST}, and the spin-coupling constants, *J*, are tabulated in Table 1. As seen from Table 1, the spin contaminations are very low for triplet states, the deviation of $\langle \hat{S}^2 \rangle$ from the expectation value of 2 is at most 0.078, whereas much higher spin contaminations are obtained for most of BS singlets, with $\langle \hat{S}^2 \rangle \approx 0.347-1.034$, except **17** and **23,** which are almost free of spin contaminations. Therefore the spin-projection procedure is necessary for eliminating spin contaminations. Because the spin-coupling constants J_{ND} and J_Y, obtained by schemes 1 and 2, respectively, are very close to each other, we only use J_Y to calculate the S−T gap (ΔE_{ST}) with Ginsberg's formula $\Delta E_{ST} = \langle \hat{S}^2 \rangle_T J_Y$.[62] Hereafter *J* means J_Y for convenience.

As shown in Table 1, the calculated results indicate that molecules of H−B−D and H−B−A types (**2**−**12**), or D−B−H and A−B−H types (**13**−**16**), all have triplet ground states although their spin-coupling constants *J* or S−T gaps are smaller than that of the parent molecule **1**. It seems clear that the spin-coupling constant decreases roughly with the increase of the strength of donors or acceptors. For example, *J* value is 6.35 for **1**, and it varies from 6.06, 5.79, 4.56, 4.61 to 3.74 with the donor substituents varying from OH, OMe, CH_3, NH_2 to NMe_2. For A−B−A (**19**, **22**) or D−B−D (**25**, **26**) types, triplet ground states with diminished *J* values are also obtained. However, for push−pull molecules of D−B−A (**17**, **18,** and **20**), or contrariwise A−B−D (**23**, **24**) types, substitutions, in sharp contrast, lead to singlet ground states or nearly degenerate ground states (i.e., a very small S−T gap). For molecules such as **21**, with a

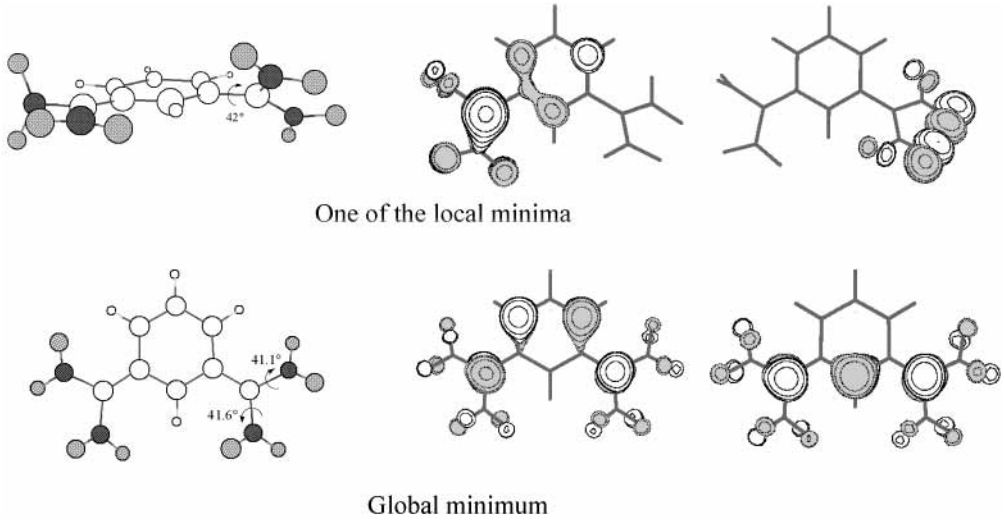

Figure 3. Global minimum structure and one of the local minimum structures for molecule **12** in the triplet state. Their SOMOs calculated by ROB3LYP in the triplet state are also given, respectively.

very small S−T gap, it might be difficult for the current DFT method to predict their ground-state spin multiplicities accurately. For example, we carry out calculations on 4,6-dimethoxy-1,3-phenylenebis(*N-tert*-butyl nitroxide) and obtain a very small *J* value (0.097 kcal/mol), but a singlet ground state was found experimentally (−0.007 kcal/mol in PVC film, −0.073 kcal/mol for its crystalline form).[41b]

One may wonder whether the calculated S−T gaps can be partially understood by the optimized UB3LYP geometries. Obviously, it is difficult to predict the magnitude or sign of the S−T gaps for different molecules by only checking their optimized structures. For example, both **15** and **17** are planar, but the S−T gap is 11.31 kcal/mol for **15**, −8.44 kcal/mol for **17**. In **25** and **26**, the nitrogen atoms of two amino groups at the radical centers have similar torsion angles, but the calculated S−T gap in **25** (11.21 kcal/mol) differs significantly from that in **26** (5.86 kcal/mol). Furthermore, even for a given molecule if the twisting of substituents out of the aromatic plane is less significant, i.e., the twisting angle is less than 30.0°, the effect of twisting the substituents on the S−T gap is insignificant. We have taken two species **3** and **12** as two examples to demonstrate this point. For both species, we have obtained their corresponding planar structures for both triplet and singlet states by performing constrained geometry optimizations. The planar structure of **3** is calculated to be 15.33 kcal/mol above the global minimum **3** shown in Figure 2, but the adiabatic S−T gap is 9.25 kcal/mol, almost identical to that obtained for **3** (9.43 kcal/mol). For **12**, its planar structure is 27.99 kcal/mol higher in energy, but the S−T gap of this planar structure (6.92 kcal/mol) is very close to that of the structure shown in Figure 2. Thus, these two cases show that twisting substituents out of conjugation by some degrees has little effect on the spacing of the singlet and the triplet state. However, if the substituents at radical centers are π-conjugated substituents and they twist severely out of the aromatic plane, the S−T gap of the substituted diradical will decrease considerably, as observed by previous works.[24a,40−44] For species **12**, we also located a local minimum structure, as displayed in Figure 3. One can see that this structure is quite different from that of the global minimum **12**. In this structure, the right radical center has both nitro groups planar, but the whole $C(NO_2)_2$ moiety is twisting 42° out of the aromatic plane, and the left radical center is almost coplanar with the aromatic plane, with one nitro group conjugated and the other out of conjugation. This structure is 13.83 kcal/mol higher in energy than that of **12**, and its S−T gap is calculated to be only 0.31 kcal/mol, much lower than that in **12** (7.67 kcal/mol). The reason behind this dramatic change is that two SOMOs in this local minimum (as seen from Figure 3) have a disjoint topology, whereas two SOMOs in the global minimum **12** are nondisjoint, similar to those in the parent diradical **1**. For diradicals, the topological character of two SOMOs is essential for understanding their S−T gaps, we will delay the discussions later in the subsequent section. Thus, this example shows that the severe twisting of substituents out of the aromatic plane may significantly decrease the S−T gap or even lead to nearly degenerate triplet and singlet states.

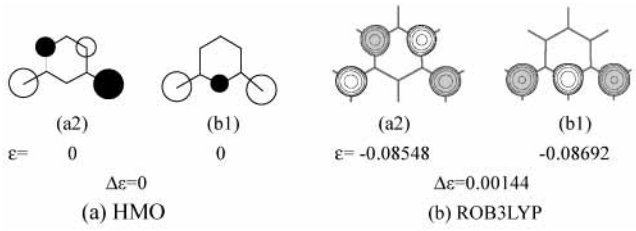

Figure 4. SOMOs of **1** and their energy levels (ϵ) (au), as well as SOMO−SOMO energy splittings ($\Delta\epsilon$) (au), by (a) HMO and (b) ROB3LYP.

The above analysis shows that for substituted diradicals the use of the geometrical arguments is not enough for understanding the dependence of the S−T gap on substituents. Now we focus on a perturbative analysis in terms of molecular orbital (MO) picture to get some qualitative understanding on the calculated results. Within the Hückel molecular orbital (HMO) theory, the nonbonding molecular orbitals (NBMOs) of **1** are sketched in Figure 4a. These two NBMOs (*a*2 and *b*1) are degenerate and have a nondisjoint topology (some atomic orbitals (AOs) are shared by both NBMOs). One SOMO has large coefficients at two radical centers, and relatively smaller coefficients at 4,6-positions of *m*-phenylene, and the other SOMO has large coefficients at two radical centers and relatively smaller coefficients at 2-position of *m*-phenylene. According to Hund's rule and Borden−Davidson's criterion,[38] an open shell singlet in which one electron occupies each of these NBMOs in opposite spin is destabilized because of large repulsions on shared AOs, and thus, a triplet ground state is obtained (hence NBMOs are singly occupied molecular orbitals, SOMOs). By performing restricted open-shell B3LYP (ROB3LYP) calcula-

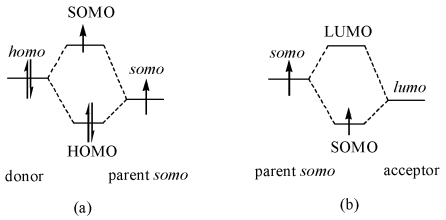

Figure 5. Schematic drawing of the interaction of the parent radical SOMO with (a) donor and (b) acceptor.

tions on the triplet state of **1**, we can obtain a more elaborate picture of the two SOMOs, as shown in Figure 4b. The two SOMOs of **1** are, of course, not exactly degenerate, but they are very close to each other, and they are topologically very similar to those obtained at HMO level.

The introduction of asymmetric perturbations (here the word "perturbation" means that they do not change the SOMOs' nodisjoint feature) to the parent diradical is expected to open up an energy gap between the SOMOs, thus diminish the singlet−triplet splitting, and even result in singlet ground states. However, one should note that the perturbative effect on the energy levels of both SOMOs by donor or acceptor substituents is quite different. A schematic depiction of one *somo* (in the parent diradical **1**) interacting with the orbitals of donor and acceptor substituents is respectively shown in Figure 5a,b. In case a, the *somo* of the parent diradical and the highest occupied molecular orbital (*homo*) of a typical donor, which is often higher in energy than the *somo* of the radical, interact mutually and the resultant SOMO is higher in energy than the *somo* in the parent diradical. In case b, the *somo* of the parent radical interacts with the lowest unoccupied molecular orbital (*lumo*) of the acceptor, which has a lower energy than the *somo* of the radical, yielding a SOMO that is lower in energy than the parent *somo*. So the introduction of electron donor or acceptor substituents into the parent diradical system will respectively lift or lower the energy level of each *somo* of the parent diradical. Furthermore, the energy lifting or lowering of the resultant SOMO would be quite significant if donor and acceptor substituents occur at those atoms having large coefficients in the *somo* of the parent diradical and would be relatively less significant if substituents are introduced into the atoms with negligible coefficients in the parent *somo*.

Let us turn to our selected diradicals. Individually, in diradicals of H−B−D and H−B−A types, four R2 groups are symmetrically introduced at the two radical sites that have large coefficients in both SOMOs, thus both SOMOs are simultaneously perturbed. It should have no strong effect on the SOMO−SOMO splitting. In D−B−H and A−B−H types, two R1 groups are introduced at the 4,6-positions of *m*-phenylene where there are larger coefficients in one SOMO (*a*2), and negligible coefficients in the other. Thus *a*2 is strongly perturbed, whereas the other is relatively weakly perturbed. This should open up larger SOMO−SOMO splittings than those in two former types. Similar effects should also be observed in molecules of D−B−A and A−B−D types.

To see how the energy levels of two SOMOs of the parent diradical are quantitatively affected by various substituents, we tabulate energy levels of two SOMOs calculated at the ROB3LYP/6-31G* level for the triplet state for all studied molecules in Table 2. For the parent diradical **1**, the SOMO−SOMO orbital energy splitting ($\Delta\epsilon$) is very small (0.00144 hartree). Clearly, the changing trend of energy levels of two SOMOs is in line with the qualitative description given above, especially in those molecules of H−B−A (or D), D−B−D, and A−B−A types. For example, the energies of two SOMOs (*a*2 and *b*1, respectively) of **1** are −0.08548 and −0.08692 au, respectively. The corresponding values become higher in molecules **3** (−0.04752, −0.04249), **13** (−0.06179, −0.07912), and **26** (−0.03579, −0.03725), with R1, R2, or both groups being NH_2 (donor substituent), and lower in molecules **12** (−0.15062, −0.15740), **16** (−0.13397, −0.11433), and **22** (−0.17885, −0.17169), with R1, R2, or both groups being NO_2 (acceptor substituent). For molecules with both donor and acceptor substituents, the substitution effect on the energy levels of both SOMOs is still obvious. For example, A−B−D type **23** can be regarded as H−B−D type **3** with two R1 groups replaced by two acceptor substituents (NO_2). Indeed, when compared to the energy levels of **3**, the corresponding values in **23** (−0.09402, −0.07193) verify the energy lowering effect of both SOMOs due to the introduction of two acceptor substituents. On the other hand, the effects of substituents on the SOMO−SOMO splittings, as seen from Table 2, are in accord with the qualitative discussions in previous paragraphs. For example, the SOMO−SOMO splitting in D−B−H type **13** (0.01733 au) and A−B−D type **23** (0.02209 au) is significantly larger than that in H−B−D type **3** (0.00503 au).

TABLE 2: Energy Levels (ϵ1 and ϵ2) and Absolute Values of Energy Splittings ($\Delta\epsilon$) of Singly Occupied Molecular Orbitals Calculated by Using ROB3LYP/6-31G(d) for the Triplet State[a]

molecules	$\epsilon 1$[b]	$\epsilon 2$[b]	$\Delta\epsilon$[b]	ΔE_{ST}[c]
1	−0.08548	−0.08692	0.00144	13.15
2	−0.04695	−0.04265	0.00430	7.64
3	−0.04752	−0.04249	0.00503	9.43
4	−0.07379	−0.07297	0.00082	9.39
5	−0.06359	−0.06066	0.00293	11.93
6	−0.06208	−0.05866	0.00342	12.48
7	−0.08495	−0.08265	0.00230	11.68
8	−0.09980	−0.10133	0.00153	9.83
9	−0.11780	−0.12381	0.00601	8.29
10	−0.14024	−0.14418	0.00394	4.88
11	−0.14468	−0.15063	0.00595	5.90
12	−0.15062	−0.15740	0.00678	7.67
13	−0.06179	−0.07912	0.01733	6.06
14	−0.06653	−0.07885	0.01232	10.13
15	−0.12305	−0.11165	0.01140	11.31
16	−0.13397	−0.11433	0.01964	3.50
17	−0.11444	−0.14019	0.02575	−8.44
18	−0.12266	−0.13930	0.01664	−0.56
19	−0.16453	−0.16366	0.00087	6.85
20	−0.13049	−0.15398	0.02349	−8.08
21	−0.13218	−0.14633	0.01415	0.51
22	−0.17885	−0.17169	0.00716	3.10
23	−0.09402	−0.07193	0.02209	−19.42
24	−0.08399	−0.06138	0.02261	−4.11
25	−0.03532	−0.03554	0.00022	11.21
26	−0.03579	−0.03725	0.00146	5.86

[a] S−T energy gaps given in Table 1 are also listed for the purpose of comparison. [b] Values are in au. [c] Values are in kcal/mol.

The analysis described above shows the effect of substituents on the energy levels of SOMOs. However, in some cases the introduction of substituents has significant influence on the spatial distributions of SOMOs. For some representative molecules we have shown their SOMOs in Figure 6. It is obvious that for those diradicals of H−B−A (or D), D−B−D, and A−B−A types their SOMOs are topologically very similar to those of the parent diradical **1** although they may have relatively smaller components at R1 or R2 substituents. These diradicals may be called typical nondisjoint diradicals for convenience in later discussions. Whereas for those push−pull diradicals of D−B−A or A−B−D type, their SOMOs are still topologically nondisjoint, but the principal components of one or two SOMOs

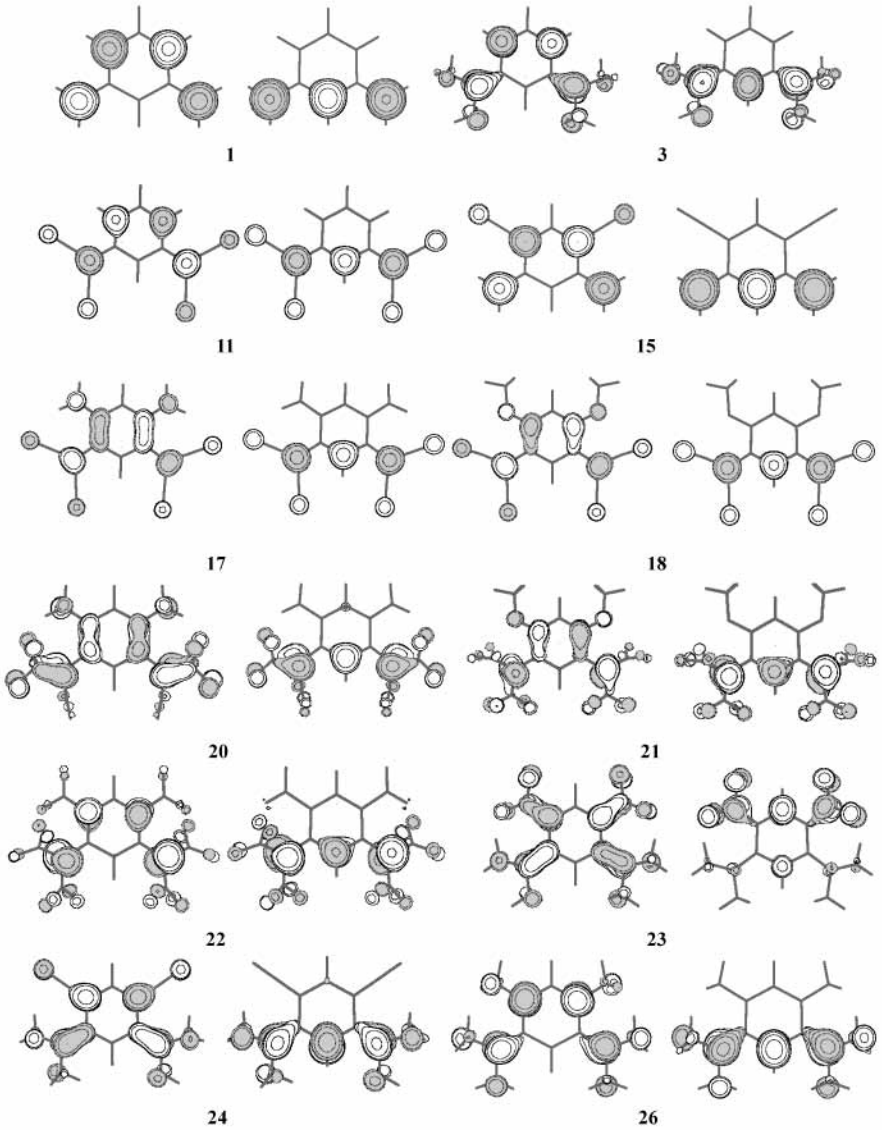

Figure 6. Contour plots of SOMOs (top view) of some representative molecules calculated by ROB3LYP in the triplet state.

are quite different from those of two SOMOs in the diradical **1**. Thus we call these diradicals nontypical nondisjoint diradicals. For example, one SOMO of **20** is similar to the *a2* SOMO of **1** in topology but it also has large coefficients at 1,3-positions of the aromatic ring, whereas for **23** its two SOMOs are spatially dramatically different from the corresponding SOMOs of **1**.

On the basis of the ROB3LYP energy levels and spatial distributions of both SOMOs for the triplet state, now we will give some qualitative discussions on the results tabulated in Table 1. First, one can see that for those typical nondisjoint diradicals such as **3** and **11** they have robust triplet ground states. Whereas for those push−pull molecules with one or two SOMOs topologically quite different from those of the parent diradical **1** like **17** and **18** they are found to have singlet ground states or nearly degenerate ground states. Thus, for substituted diradicals the topological features of their SOMOs are found to be the most important factor for determining the ground-state multiplicities.

Second, for a homologous series of typical nondisjoint diradicals their S−T gaps are closely related to the calculated splitting of two SOMOs according to Borden−Davidsion's rule.[38] From Table 2 and the plot of S−T gaps vs SOMO−SOMO splittings ($\Delta\epsilon$) (Figure 7, several nontypical nondisjoint diradicals are excluded), it seems that in most cases a smaller SOMO−SOMO splitting is likely to give rise to a larger S−T gap, although there is not a clear proportion between the splittings of SOMOs and S−T gap values. For instance, for molecules **1**−**12** of H−B−D and H−B−A types their SOMO−SOMO splittings are quite small, thus they are found to have triplet ground states with significant S−T gaps.

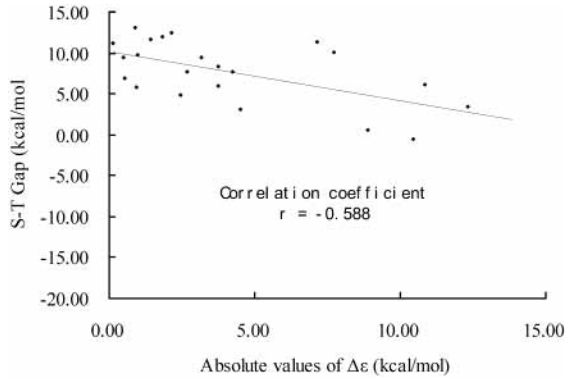

Figure 7. UB3LYP S−T gaps vs the absolute values of SOMO−SOMO splittings $\Delta\epsilon$ calculated with ROB3LYP for the triplet state in studied typical nondisjoint diradicals.

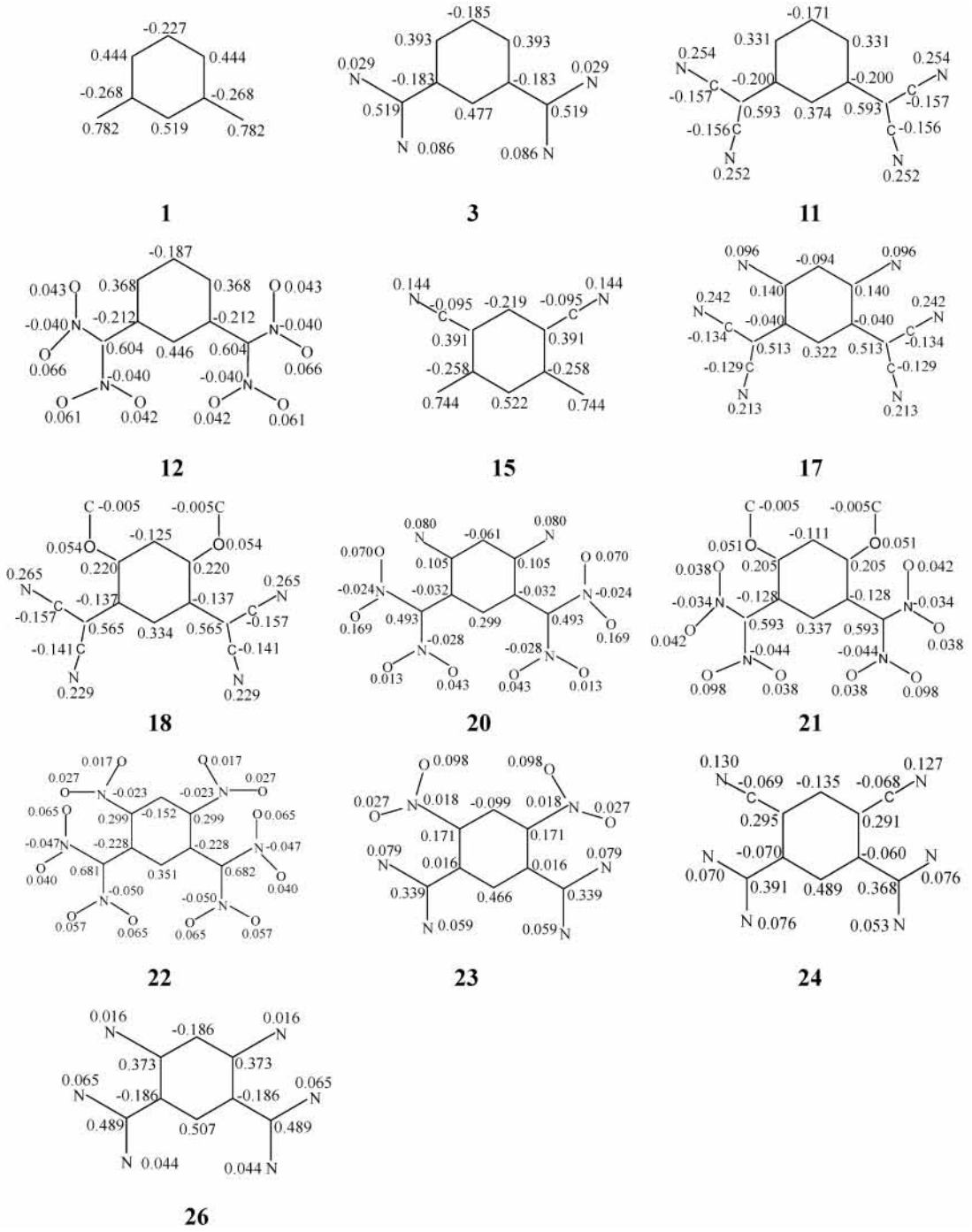

Figure 8. Population of spin densities for triplet states of some representative molecules calculated by UB3LYP/6-31G(d) (hydrogen atoms are omitted for clarity).

Third, it can be seen that even for typical nondisjoint diradicals their S−T gaps depend on, to a considerable degree, the extent which SOMOs overlap in space. For example, two SOMOs in each of **11** and **15** are typically nondisjoint (as shown in Figure 6). Like the parent **1**, two SOMOs in **15** have large coefficients at two radical centers, leading to the large repulsions, and thus a larger S−T gap. But both SOMOs in **11** are more delocalized into the regions of AOs in four CN groups, and thus are substantially coextensive in space. Thus two electrons with antiparallel spins would have more chance to escape away from each other in the shared regions, resulting in lower repulsions. As a result, **11** has a smaller S−T gap than **15**, although the SOMO−SOMO splitting in **15** (0.01140 au) is larger than that in **11** (0.00595 au).

Fourth, when splittings of SOMOs are relatively large, either very small positive S−T gaps are obtained (e.g., **16** and **21**), or even the sign of the S−T gap value is inverted (thus singlet ground states are obtained). Diradicals such as **17**, **20**, **23**, and **24** of either D−B−A or A−B−D types provide such examples. They are all nontypical nondisjoint diradicals and have SOMO−SOMO splittings larger than 0.020 au, and thus UB3LYP calculations reveal that they have singlet ground states.

Summarizing above discussions, one can see that a perturbative analysis based on the ROB3LYP energy levels and spatial distributions of two SOMOs obtained for the triplet state is very helpful for us to understand the spin coupling in studied diradicals. On the other hand, we feel that the population of spin densities in the triplet state may provide further support to

our above-described analysis. Figure 8 gives schematic illustrations of the population of spin densities of some representative molecules calculated by the UB3LYP method in triplet states. As illustrated in Figure 8, the parent **1** has an alternate distribution of spin densities, and so do **11** and **15** with R1 or R2 acceptor substituents (CN). This is in conformity with the spin polarization effect[52a,65] through *m*-phenylene via the π-network, being characteristic of a triplet ground state. As pointed out in above discussions, two SOMOs in **11** are much more delocalized than those in **15**. This is confirmed by calculated spin densities, which show stronger spin delocalization effects in **11** than those in **15**.

However, one can see that the spin alternation rule is broken down to some extent in diradicals with very small S−T gaps such as **18** and **21** but is severely violated in diradicals with singlet ground states such as **17**, **20**, **23**, and **24**. For example, in **18** and **21** the spin densities on the carbons (C4 or C6) of the *m*-phenylene and the connected oxygen atom of OMe substituent have the same sign. For diradicals with singlet ground states, a common feature of these diradicals is that they have negligible spin densities on carbons (C1 and C3) of *m*-phenylene connected to the radical sites (e.g., −0.032, −0.032 for **20**). Meanwhile, the spin densities in these molecules are significantly delocalized into external donor and acceptor substituents, leading to smaller spin populations on carbon radical centers (C7 and C8) (e.g., 0.493, 0.493 for species **20**). Thus, by checking the UB3LYP spin densities calculated for the triplet state of a diradical, one is also able to give a qualitative estimate on whether a diradical is a robust triplet state or not (without performing calculations for the singlet state).

4. Conclusion

The lowest singlet and triplet states of a series of *m*-phenylene-bridged diradicals with various substituents have been studied by using UB3LYP calculations with the spin-projection procedure to investigate the effects of substitution on the singlet−triplet energy gaps and the ground-state spin multiplicities. Our calculations show that the introduction of electron-donating (or electron-withdrawing) substituents on the 4,6-positions of the *m*-phenylene moiety or on the radical centers, or on both positions, generally leads to a triplet ground state, although the singlet−triplet energy gaps are smaller than that of the parent *m*-xylylene diradical to some extent. However, the simultaneous substitution of electron-donating and electron-withdrawing groups at *m*-phenylene and radical centers, and vice versa, will result in a singlet ground state or a very small positive S−T gap. Using the ROB3LYP SOMOs and the UB3LYP spin densities obtained for the triplet state, we have shown that the ground-state multiplicity in studied diradicals can be well interpreted by the spatial distributions of SOMOs, but the S−T gap is found to depend on both the spatial distributions of SOMOs and the SOMO−SOMO energy splittings.

Acknowledgment. This work was supported by the National Natural Science Foundation of China (Grant No. 20073020). We are grateful to the referees for their pertinent comments and good suggestions concerning our original manuscript. Partial computations are carried out on the SGI Origin 3800 and Dawning 3000A at Nanjing University.

References and Notes

(1) Dougherty, D. A. *Acc. Chem. Res.* **1991**, *24*, 88−94.
(2) Rajca, A. *Chem. Rev.* **1994**, *94*, 871−893.
(3) Miller, J. S.; Epstein, A. J. *Angew. Chem. Int. Ed. Engl.* **1994**, *33*, 385−415.
(4) *Magnetic Properties of Organic Materials*; Lathi, P. M., Ed.; Marcel Dekker: New York, 1999.
(5) Miller, J. S. *Inorg. Chem.* **2000**, *39*, 4392−4408.
(6) Crayston, J. A.; Devine, J. N.; Walton, J. C. *Tetrahedron* **2000**, *56*, 7829−7857.
(7) (a) Dougherty, D. A. *Mol. Cryst. Liq. Cryst.* **1989**, *176*, 25−32. (b) Dougherty, D. A. *Mol. Cryst. Liq. Cryst.* **1990**, *183*, 71−79. (c) Silverman, S. K.; Dougherty, D. A. *J. Phys. Chem.* **1993**, *97*, 13273.
(8) Mataga, N. *Theor. Chim. Acta* **1968**, *10*, 372−376.
(9) Schlenk, W.; Brauns, M. *Ber. Dtsch. Chem. Ges.* **1915**, *48*, 661−669.
(10) Kothe, G.; Denkel, K. H.; Summermann, W. *Angew. Chem., Int. Ed. Engl.* **1970**, *9*, 906−907.
(11) (a) Itoh, K. *Chem. Phys. Lett.* **1967**, *1*, 235. (b) Wasserman, E.; Murray, R. W.; Yager, W. A.; Trozzolo, A. M.; Smolinsky, G. J. *J. Am. Chem. Soc.* **1967**, *89*, 5076−5078.
(12) (a) Haider, K.; Soundararajan, N.; Shaffer, M.; Platz, M. S. *Tetrahedron Lett.* **1989**, *30*, 1225−1228. (b) Fukuzawa, T. A.; Sato, K.; Ichimura, A. S.; Kinoshita, T.; Takui, T.; Itoh, K.; Lahti, P. M. *Mol. Cryst. Liq. Cryst.* **1996**, *278*, 253−260.
(13) (a) Calder, A.; Forrester, A. R.; James, P. G.; Luckhurst, G. R. *J. Am. Chem. Soc.* **1969**, *91*, 3724−3727. (b) Ishida, T.; Iwamura, H. *J. Am. Chem. Soc.* **1991**, *113*, 4238−4241.
(14) Sugawara, T.; Bandow, S.; Kimura, K.; Iwamura, H.; Itoh, K. *J. Am. Chem. Soc.* **1986**, *108*, 368−371.
(15) Teki, Y.; Takui, T.; Itoh, K.; Iwamura, H.; Kobayashi, K. *J. Am. Chem. Soc.* **1986**, *108*, 2147−2156.
(16) Iwamura, H. *Pure Appl. Chem.* **1993**, *65*, 57−64.
(17) Matsuda, K.; Nakamura, N.; Takahashi, K.; Inoue, K.; Koga, N.; Iwamura, H. *J. Am. Chem. Soc.* **1995**, *117*, 5550−5560.
(18) (a) Rajca, A.; Utamapanya, S.; Xu, J. *J. Am. Chem. Soc.* **1991**, *113*, 9235−9241. (b) Rajca, A.; Utamapanya, S. *J. Org. Chem.* **1992**, *57*, 1760−1767. (c) Utamapanya, S.; Rajca, A. *J. Am. Chem. Soc.* **1991**, *113*, 9242−9251.
(19) (a) Rajca, A.; Utamapanya, S. *J. Am. Chem. Soc.* **1993**, *115*, 2396−2401. (b) Rajca, A.; Utamapanya, S. *J. Am. Chem. Soc.* **1993**, *115*, 10688−10694.
(20) Veciana, J.; Rovira, C.; Crespo, M. I.; Armet, O.; Domingo, V. M.; Palacio, F. *J. Am. Chem. Soc.* **1991**, *113*, 2552−2561.
(21) (a) Sato, K.; Yano, M.; Furuichi, M.; Shiomi, D.; Takui, T.; Abe, K.; Itoh, K.; Higuchi, A.; Katsuma, K.; Shirota, Y. *J. Am. Chem. Soc.* **1997**, *119*, 6607−6613. (b) Stickley, K. R.; Selby, T. D.; Blackstock, S. C. *J. Org. Chem.* **1997**, *62*, 448−449. (c) Murray, M. M.; Kaszynski, P.; Kaisaki, D. A.; Chang W.; Dougherty, D. A. *J. Am. Chem. Soc.* **1994**, *116*, 8152−8161.
(22) Gajewski, J. J.; Gitendra, C. P. *Tetrahedron Lett.* **1998**, *39*, 351−354.
(23) Itoh, K. *Pure Appl. Chem.* **1978**, *50*, 1251−1259.
(24) (a) Silver S. K.; Dougherty, D. A. *J. Phys. Chem.* **1993**, *97*, 13273−13283. (b) Jacobs, S. J.; Shuitz, D. A.; Jain, R.; Novak, J.; Dougherty, D. A. *J. Am. Chem. Soc.* **1993**, *115*, 1744−1753. (c) West, A. P., Jr.; Silverman, S. K.; Dougherty, D. A. *J. Am. Chem. Soc.* **1996**, *118*, 1452−1463.
(25) Yoshizawa, K.; Kuga, T.; Sato, T.; Hatanaka, M; Tanaka, K.; Yamabe, T. *Bull. Chem. Soc. Jpn.* **1996**, *69*, 3443−3450.
(26) Mitani, M.; Yamaki, D.; Yoshioka, Y.; Yamaguchi, K. *J. Chem. Phys.* **1999**, *111*, 2283−2294.
(27) Mitani, M.; Mori, H.; Takano, Y.; Yamaki, D.; Yoshioka, Y.; Yamaguchi, K. *J. Chem. Phys.* **2000**, *113*, 4035−4051.
(28) Mitani, M.; Yamaki, D.; Takano, Y.; Kitagawa, Y.; Yoshioka, Y.; Yamaguchi, K. *J. Chem. Phys.* **2000**, *113*, 10486−10504.
(29) Mitani, M.; Takano, Y.; Yoshioka, Y.; Yamaguchi, K. *J. Chem. Phys.* **1999**, *111*, 1309−1324.
(30) Migirdicyan, E.; Bauder, J. *J. Am. Chem. Soc.* **1975**, *97*, 7400−7404.
(31) Wenthold, P. G.; Kim J. B.; Lineberger, W. C. *J. Am. Chem. Soc.* **1997**, *119*, 1354−1359 and references therein.
(32) Kato, S.; Morokuma, K.; Feller, D.; Davidson E. R.; Borden, W. T. *J. Am. Chem. Soc.* **1983**, *105*, 1791−1795.
(33) Fort, R. C., Jr.; Getty, S. J.; Hrovat, D. A.; Lahti P. M.; Borden, W. T. *J. Am. Chem. Soc.* **1992**, *114*, 7549−7552.
(34) Iwase, K.; Inagaki, S. *Bull. Chem. Soc. Jpn.* **1996**, *69*, 2781−2789.
(35) Hrovat, D. A.; Murcko, M. A.; Lahti P. M.; Borden, W. T. *J. Chem. Soc., Perkin Trans. 2* **1998**, 1037−1044.
(36) Havlas, Z.; Michl, J. *J. Chem. Soc., Perkin Trans. 2* **1999**, 2299−2303.
(37) Longuet-Higgins, H. C. *J. Chem. Phys.* **1950**, *18*, 265−274.
(38) (a) Borden, W. T.; Davidson, E. R. *J. Am. Chem. Soc.* **1977**, *99*, 4587−4594. (b) Borden, W. T. In *Magnetic Properties of Organic Materials*; Lahti, P. M., Ed.; Marcel Dekker: New York, 1999; pp 61−102.
(39) Ovchinnikov, A. A. *Thror. Chim. Acta* **1978**, *47*, 297−304.

(40) Shultz, D. A. In *Magnetic Properties of Organic Materials*; Lahti, P. M., Ed.; Marcel Dekker: New York, 1999; pp 103−125.

(41) (a) Dvolaitzky, M.; Chiarelli, R.; Rassat, A. *Angew. Chem., Int. Ed. Engl*. **1992**, *31*, 180−181. (b) Kanno, F.; Inoue, K.; Koga, N.; Iwamura, H. *J. Am. Chem. Soc.* **1993**, *115*, 847−850. (c) Fujita, J.; Tanaka, M.; Suemune, H.; Koga, N.; Matsuda, K.; Iwamura, H. *J. Am. Chem. Soc.* **1996**, *118*, 9347−9351.

(42) (a) Okada, K.; Imakura, T.; Oda, M.; Murai, H. *J. Am. Chem. Soc.* **1996**, *118*, 3047−3048. (b) Okada, K.; Imakura, T.; Oda, M.; Kajiwara, A.; Kamachi, M.; Yamaguchi, M. *J. Am. Chem. Soc.* **1997**, *119*, 5740−5741.

(43) Fang, S.; Lee, M. S.; Hrovat, D. A.; Borden, W. T. *J. Am. Chem. Soc.* **1995**, *117*, 6727−6731.

(44) Rajca, A.; Rajca, S. *J. Chem. Soc., Perkin Trans. 2* **1998**, 1077−1082.

(45) (a) Dowd, P. *J. Am. Chem. Soc.* **1966**, *88*, 2587−2589. (b) Platz, M. S.; McBride, J. M.; Little, R. D.; Harrison, J. J.; Shaw, A.; Potter, S. E.; Berson, J. A. *J. Am. Chem. Soc.* **1976**, *98*, 5725−5726. (c) Baseman, R. J.; Pratt, D. W.; Chow, M.; Dowd, P. *J. Am. Chem. Soc.* **1976**, *98*, 5726−5727. (d) Wenthold, P. G.; Hu, J.; Squires, R. R.; Lineberger, W. C. *J. Am. Chem. Soc.* **1996**, *118*, 475−476. (e) Wenthold, P. G.; Hu, J.; Squires, R. R.; Lineberger, W. C. *J. Am. Soc. Mass Spectrom.* **1999**, *10*, 800−809.

(46) Coolidge, M. B.; Yamashita, K.; Morokuma, K.; Borden, W. T. *J. Am. Chem. Soc.* **1990**, *112*, 1751−1754.

(47) (a) Hirano, T.; Kumagai, T.; Miyashi, T.; Akiyama, K.; Ikegami, Y. *J. Org. Chem.* **1991**, *56*, 1907−1914. (b) Ichimura, A. S.; Lahti, P. M.; Matlin, A. R. *J. Am. Chem. Soc.* **1990**, *112*, 2868−2875. (c) Powell, H. K.; Borden, W. T. *J. Org. Chem.* **1995**, *60*, 2654−2655. (d) Lahti, P. M.; Rossi, A. R.; Berson, J. A. *J. Am. Chem. Soc.* **1985**, *107*, 2273−2280.

(48) (a) Du, P.; Hrovat, D. A.; Borden, W. T. *J. Am. Chem. Soc.* **1989**, *111*, 3773−3778. (b) Du, P.; Hrovat, D. A.; Borden, W. T. *J. Am. Chem. Soc.* **1986**, *108*, 8086−8087. (c) Nash, J. J.; Dowd, P.; Jordan, K. D. *J. Am. Chem. Soc.* **1992**, *114*, 10071−10072.

(49) (a) Becke, A. D. *J. Chem. Phys.* **1993**, 98, 5648−5652. (b) Lee, C.; Yang, W.; Parr, R. G. *Phys. Rev. B* **1988**, *37*, 785−789.

(50) (a) Yamaguchi, K.; Fueno, T. *Chem. Phys. Lett.* **1973**, *22*, 461−465. (b) Yamaguchi, K. *Chem. Phys. Lett.* **1975**, *33*, 330−335. (c) Yamaguchi, K. *Chem. Phys. Lett.* **1979**, *66*, 395−399. (d) Benard, M. *J. Chem. Phys.* **1979**, 71, 2546−2556.

(51) (a) Noodleman, L. *J. Chem. Phys.* **1981**, *74*, 5737−5743. (b) Noodleman, L.; Davidson, R. *Chem. Phys.* **1986**, *109*, 131−143.

(52) (a) Yamaguchi, K.; Toyoda, Y.; Fueno, T. *Synth. Met*. **1987**, *19*, 81. (b) Yamanaka, S.; Okumura, M.; Yamaguchi, K.; Hirao, K. *Chem. Phys. Lett.* **1994**, *225*, 213−220. (c) Yamanaka, S.; Kawakami, T.; Nagao, H.; Yamaguchi, K. *Chem. Phys. Lett.* **1994**, *231*, 25−33.

(53) (a) Takano, Y.; Soda, T.; Kitagawa, Y.; Yoshioka, Y.; Yamaguchi, K. *Chem. Phys. Lett*. **1999**, 301, 309−316. (b) Soda, T.; Kitagawa, Y.; Onishi, T.; Takano, Y.; Shigeta, Y.; Nagao, H.; Yoshioka, Y.; Yamaguchi, K. *Chem. Phys. Lett*. **2000**, 319, 223−230. (c) Takano, Y.; Kubo, S.; Onishi, T.; Isobe, H.; Yoshioka, Y.; Yamaguchi, K. *Chem. Phys. Lett*. **2001**, 335, 395−403.

(54) Yamaguchi, K.; Okumura, M.; Takada K.; Yamanaka, S. *Int. J. Quantum Chem. Symp*. **1993**, *27*, 501−515.

(55) (a) Yamaguchi, K.; Jensen, F.; Dorigo, A.; Houk K. N. *Chem. Phys. Lett*. **1988**, 149, 537−542. (b) Yamaguchi, K. Takahara, Y.; Fueno, T.; Houk, K. N. *Theor. Chim. Acta* **1988**, *73*, 337−364.

(56) Kemnitz, C. R.; Squires, R. R.; Borden, W. T. *J. Am. Chem. Soc.* **1997**, *119*, 6564−6574.

(57) Lahti, P. M.; Ichimura, A. S.; Sanborn, J. A. *J. Phys. Chem. A* **2001**, *105*, 251−260.

(58) Adamo, C.; di Matteo, A.; Barone, V. *Adv. Quantum Chem.* **1999**, *36*, 45−75.

(59) Strassner, T.; Weitz, A.; Rose, J.; Wudl, F.; Houk, K. N. *Chem. Phys. Lett*. **2000**, *321*, 459−462.

(60) Takano, Y.; Onishi, T.; Kitagawa, Y.; Soda, T.; Yoshioka, Y.; Yamaguchi, K. *Int. J. Quantum Chem*. **2000**, *80*, 681−691.

(61) Leach, A. G.; Catak, S.; Houk, K. N. *Chem. Eur. J*. **2002**, *8*, 1290−1299.

(62) Ginsberg, A. P. *J. Am. Chem. Soc.* **1980**, *102*, 111−117.

(63) Frisch, M. J.; Trucks, G. W.; Schlegel, H. B.; Scuseria, G. E.; Robb, M. A.; Cheeseman, J. R. Zakrzewski, V. G.; Montgomery, J. A., Jr.; Stratmann, R. E.; Burant, J. C.; Dapprich, S.; Millam, J. M.; Daniels, A. D.; Kudin, K. N.; Strain, M. C.; Farkas, O.; Tomasi, J.; Barone, V.; Cossi, M.; Cammi, R.; Mennucci, B.; Pomelli, C.; Adamo, C.; Clifford, S.; Ochterski, J.; Petersson, G. A.; Ayala, P. Y.; Cui, Q.; Morokuma, K.; Malick, D. K.; Rabuck, A. D.; Raghavachari, K.; Foresman, J. B.; Cioslowski, J.; Ortiz, J. V.; Baboul, A. G.; Stefanov, B. B.; Liu, G.; Liashenko, A.; Piskorz, P.; Komaromi, I.; Gomperts, R.; Martin, R. L.; Fox, D. J.; Keith, T.; Al-Laham, M. A.; Peng, C. Y.; Nanayakkara, A.; Challacombe, M.; Gill, P. M. W.; Johnson, B.; Chen, W.; Wong, M. W.; Andres, J. L.; Gonzalez, C.; Head-Gordon, M.; Replogle, E. S.; Pople, J. A. *Gaussian 98*, release A.9; Gaussian, Inc.: Pittsburgh, PA, 1998.

(64) Goldstein, E.; Beno, Brett; Houk, K. N. *J. Am. Chem. Soc.* **1996**, *118*, 6036−6043.

(65) Yamaguchi, K.; Okumura, M.; Maki, J.; Noro, T. *Chem. Phys. Lett*. **1993**, *207*, 9−14.